

Time-dependent CP violation in B decays at Belle

Yosuke Yusa*

Niigata University

E-mail: yusa@hep.sc.niigata-u.ac.jp

Using the entire Belle dataset collected at the $\Upsilon(4S)$ resonance containing 772 million B -meson pairs, measurements of time-dependent CP violation in neutral B meson decays are performed for the decay channels governed by, or sensitive to, the $b \rightarrow s$ penguin (loop) transitions. In this presentation, we report recent measurement of CP violation parameters.

*European Physical Society Conference on High Energy Physics - EPS-HEP2019 -
10-17 July, 2019
Ghent, Belgium*

*Speaker.

In the Standard Model (SM), CP violation of the quark sector is induced if the complex phase appearing in the CKM matrix which describes the quark mixing [1]. Considering the unitarity between the matrix components in the system containing the b -quark, $V_{ud}V_{ub}^* + V_{cd}V_{cb}^* + V_{td}V_{tb}^* = 0$, the CP violation is parameterized as non-zero angles of the unitary triangle, $\phi_1 = \arg[-V_{cd}V_{cb}^*/V_{td}V_{tb}^*]$, $\phi_2 = \arg[-V_{ud}V_{ub}^*/V_{td}V_{tb}^*]$ and $\phi_3 = \arg[-V_{cd}V_{cb}^*/V_{ud}V_{ub}^*]$ [2]. Time-dependent CP violation is induced by quantum interference between amplitudes of decay to the CP -eigenstate through the mixing of B^0 and \bar{B}^0 induced by box diagram and that without mixing. For decays of B^0 and \bar{B}^0 mesons produced via $\Upsilon(4S) \rightarrow B\bar{B}$ transitions, the decay rate has a time dependence [3, 4]

$$\mathcal{P}(\Delta t, q) = \frac{e^{-|\Delta t|/\tau_{B^0}}}{4\tau_{B^0}} \times \left(1 + q[\mathcal{S} \sin(\Delta m_d \Delta t) + \mathcal{A} \cos(\Delta m_d \Delta t)] \right), \quad (1)$$

where \mathcal{S} and \mathcal{A} are CP -violating parameters; $q = 1$ for B^0 decays and -1 for \bar{B}^0 decays; Δt is the difference in decay times of the B^0 and \bar{B}^0 mesons; Δm_d is the mass difference between the two mass eigenstates of the B^0 - \bar{B}^0 system; and τ_{B^0} is the B^0 lifetime. In this report, we present the results of the CP violation measurement using $772 \times 10^6 B\bar{B}$ pairs accumulated with the Belle detector [5] on the $\Upsilon(4S)$ resonance at the asymmetric energy collision of 8.0 GeV e^- and 3.5 GeV e^+ at the KEKB storage ring [6].

1. Belle detector

The Belle detector is a large-solid-angle magnetic spectrometer that consists of a silicon vertex detector (SVD), a 50-layer central drift chamber (CDC), an array of aerogel threshold Cherenkov counters (ACC), a barrel-like arrangement of time-of-flight scintillation counters (TOF), and an electromagnetic calorimeter comprised of CsI(Tl) crystals (ECL) located inside a super-conducting solenoid coil that provides a 1.5 T magnetic field. An iron flux-return located outside of the coil is instrumented to detect K_L^0 mesons and to identify muons (KLM). The detector is described in detail elsewhere [5]. Two inner detector configurations were used. A 2.0 cm radius beampipe and a 3-layer silicon vertex detector was used for the first sample of $152 \times 10^6 B\bar{B}$ pairs, while a 1.5 cm radius beampipe, a 4-layer silicon detector and a small-cell inner drift chamber were used to record the remaining $620 \times 10^6 B\bar{B}$ pairs [7].

2. Analysis of the CP violation measurement

In the studies of the CP violation, we reconstruct the decay into the CP -eigenstate. Mother B^0 meson is selected by kinematic variables calculated using the information such as momentum, energy and particle identification from the Belle detector. For the kinematic variables, beam constrained mass $M_{bc} \equiv \sqrt{(E_{\text{beam}}/c^2)^2 - |\vec{p}_B^{\text{CM}}/c|^2}$ and energy difference $\Delta E \equiv E_{\text{beam}} - E_B^{\text{CM}}$ are used, where \vec{p}_B^{CM} and E_B^{CM} are B momentum and energy in the $\Upsilon(4S)$ center-of-mass system (CMS), respectively. E_{beam} is a measured beam energy in CMS. To suppress $e^+e^- \rightarrow q\bar{q}$ continuum background events, a likelihood ratio is calculated using modified Fox-Wolfram moments [8, 9] and the cosine of the angle between the beam direction and B^0 flight direction in the CMS, $\cos \theta_B$. In some of the analysis, continuum rejection is done using neural-net instead of the likelihood based

selection [10]. For the determination of the selection criteria, Monte Carlo simulated events (MC) are used. The signal sample is generated using the EVTGEN [11] hadronic event generator package. For the background, a large number of $B\bar{B}$ and $q\bar{q}$ processes are simulated. Interactions of the particles in the Belle detector are reproduced using GEANT3 [12] with detector configuration information in each time period of the experiment.

Since the B^0 flavor q is not specified from observed decay products of the CP -eigenstates, q is determined using the information of inclusive properties of particles that are not associated with the signal B^0 candidate after the selection. For the determination, a multi-dimensional likelihood based method is used [13]. The quality of the flavor tagging result is expressed by r , where $r = 0$ corresponds to no flavor discrimination, and $r = 1$ corresponds to unambiguous flavor assignment. Candidates with $r \leq 0.1$ are not used for CP violation measurement. The wrong tag fractions for six r intervals, $w_l (l = 1 - 6)$ and their difference between B^0 and \bar{B}^0 decays, Δw_l are determined from a large number of control sample B^0 decay data in which the flavor is specified by itself. The total effective tagging efficiency defined as $\Sigma(f_l \times (1 - 2w_l)^2)$ is determined to be $(29.8 \pm 0.4)\%$, where f_l is the fraction of the events in the l -th interval.

Due to the asymmetric energies of the e^+ and e^- beams, the $\Upsilon(4S)$ is produced with a Lorentz boost of $\beta\gamma = 0.425$ nearly along the $+z$ axis, which is defined as the direction opposite the e^+ beam. Since the $B^0\bar{B}^0$ pair is almost at rest in the $\Upsilon(4S)$ CMS, the decay time difference Δt can be determined from the separation along z of the B^0 and \bar{B}^0 decay vertices: $\Delta t \approx \Delta z / (\beta\gamma c)$. The vertex positions of the CP and opposite-side are reconstructed from all charged tracks in the event using a vertex reconstruction algorithm described in [14].

To measure the CP violation parameters, an unbinned maximum likelihood fit is performed for Δt and q using the signal fraction evaluated from the signal extraction fit for variables of kinematic and continuum suppression. The PDF for the signal is set to take the form of Eq. 2.1 which is obtained by modifying Eq. 1 for wrong-tagging and vertex resolution:

$$\mathcal{P}(\Delta t, q) = \frac{e^{-|\Delta t|/\tau_{B^0}}}{4\tau_{B^0}} \left(1 - q\Delta w + (1 - 2w)q [\mathcal{S} \sin(\Delta m_d \Delta t) + \mathcal{A} \cos(\Delta m_d \Delta t)] \right) \otimes R(\Delta t), \quad (2.1)$$

where $R(\Delta t)$ is a convolved resolution function which consists of components of detector resolution for z_{CP} and z_{tag} vertices, the shift of z_{tag} due to secondary tracks from long-lived particles, and kinematic approximation in the Δt calculation from vertex positions. These are determined using a large CP -conserving sample of semi-leptonic and hadronic B decays. For the background, which includes both $q\bar{q}$ and $B\bar{B}$, the PDF is modeled as a combination of two Gaussian functions and a δ -function determined using the data sample from the sideband regions of M_{bc} and ΔE . In the PDF, τ_{B^0} and Δm_d are fixed to the world average values [15] including modifications to account for the effect of an incorrect flavor assignment. In addition to the signal and background, a broad Gaussian function is included to represent a small outlier component.

3. $\sin 2\phi_1$ measurement in $B^0 \rightarrow J/\psi\pi^0$ decay

Main contribution for the $B^0 \rightarrow J/\psi\pi^0$ decay is $b \rightarrow c\bar{c}d$ tree diagram. Therefore, $S = -\sin 2\phi_1$ and $A = 0$ is expected if no extra CP violation phase from penguin diagram does not contribute [17] so that it is a probe to search new physics. On the other hand, contribution of

SM penguin diagram to $\sin 2\phi_1$ can be estimated using this decay since tree contribution is relatively small due to Cabibbo-suppression. It contributes to reduce uncertainty in measurement using $B^0 \rightarrow J/\psi K^0$ decay without model-dependence. We obtain signal yield of 332 ± 22 and determine branching fraction as $(1.62 \pm 0.11(\text{stat.}) \pm 0.06(\text{syst.})) \times 10^{-5}$. Using the sample, $\mathcal{S} = -0.59 \pm 0.19(\text{stat.}) \pm 0.03(\text{syst.})$ and $\mathcal{A} = -0.15 \pm 0.14(\text{stat.})_{-0.04}^{+0.03}(\text{syst.})$ are obtained. We obtain evidence of non-zero \mathcal{S} with significance of 3.0σ and it is consistent with SM expectation.

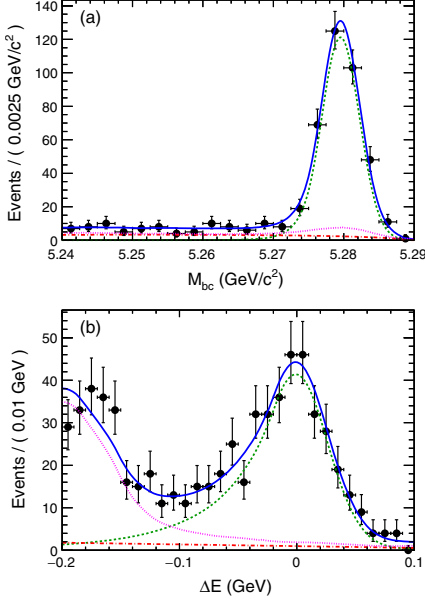


Figure 1: Distributions of M_{bc} (a) and ΔE (b) for selected $B^0 \rightarrow J/\psi\pi^0$ candidates. Points with error bars show the data and solid curve shows the fit result for signal yield extraction. Dashed curves show the signal, the dotted-dashed curves show the $q\bar{q}$ background, the dotted curves show the $B\bar{B}$ background PDF.

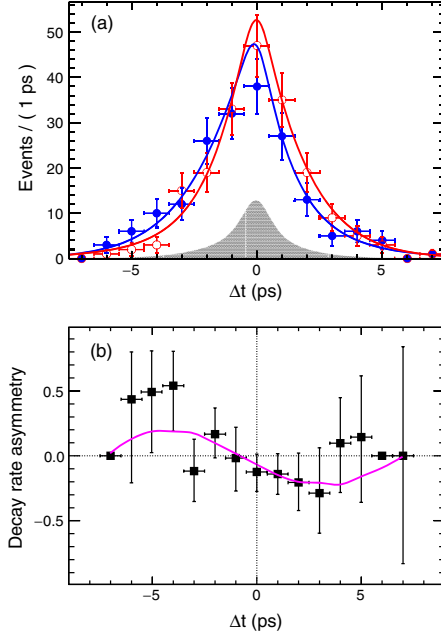


Figure 2: Δt distribution of $B^0 \rightarrow J/\psi\pi^0$ candidates (a) and decay rate asymmetry (b). Points with errors show the data and events tagged as $q = +1$ and $q = -1$ are shown with filled and open circles together with the fit curves.

4. $\sin 2\phi_1^{\text{eff}}$ measurement in CP -even states of $B^0 \rightarrow \pi^0\pi^0 K_S^0$ decay

A value of $\sin 2\phi_1$ measured in the decays induced by $b \rightarrow sq\bar{q}$ ($q = u, d, s$) penguin diagram, $\sin 2\phi_1^{\text{eff}}$, is sensitive to the new physics beyond the SM since the contribution from the new physics is expected to the loop in the diagram. We have measured several kinds of the CP -eigenstates [16] and most of the sensitivity is from the CP -odd eigenstates of $(q\bar{q})K_S^0$. Time-dependent CP violation in the CP -even states is measured only in the decays $B^0 \rightarrow \eta' K_L^0$ and $B^0 \rightarrow \phi K_L^0$ since reconstruction of the B^0 decays including the K_L^0 is difficult. $B^0 \rightarrow \pi^0\pi^0 K_S^0$ three-body decay proceeds mainly via a $b \rightarrow sdd$ “penguin” amplitude [18] and final state is CP -even followed by the K_S^0 . We note that there is a $b \rightarrow u\bar{u}s$ tree amplitude that also contributes to $B^0 \rightarrow K_S^0\pi^0\pi^0$ decays and can shift ϕ_1^{eff} from ϕ_1 ; however, this amplitude is doubly Cabibbo-suppressed, and thus the resulting shift is very small [20]. Previously, the BABAR experiment studied this decay and

measured $\sin 2\phi_1^{\text{eff}} = -0.72 \pm 0.71 \pm 0.08$ [21]; the sign is opposite to the expectation from the SM although the statistic uncertainty is large.

Since no charged tracks from the decay point of the B^0 decaying into CP eigenstate, the vertex is determined from the direction of the K_S^0 and constraint from e^+e^- interaction point. Signal yield with the vertex information of 146.7 ± 23.6 events are obtained from the three-dimensional fit to variables of kinematic and continuum suppression as shown in Figure 3. Using the selected sample, $\sin 2\phi_1^{\text{eff}} = 0.92_{-0.31}^{+0.27}(\text{stat.}) \pm 0.11(\text{syst.})$ and $\mathcal{A} = 0.28(\text{stat.}) \pm 0.04(\text{syst.})$ are obtained as shown in Figure 4. This is the first result of CP violation measurement in this decay from the Belle experiment and consistent with the SM expectation.

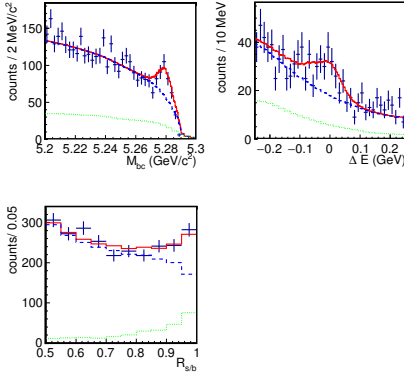


Figure 3: Distributions of M_{bc} , ΔE and modified Fox-Wolfram moments $R_{s/b}$ for selected $B^0 \rightarrow \pi^0 \pi^0 K_S^0$ candidates. Points with error bars show the data and solid curve shows the fit result for signal yield extraction. Dashed and dotted curves show the contribution of total and $B\bar{B}$ background, respectively.

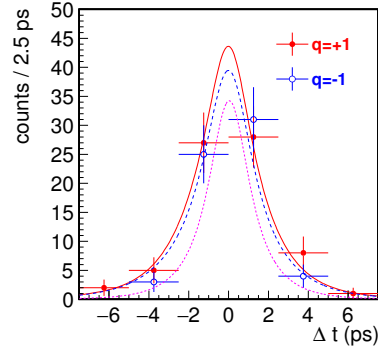


Figure 4: Δt distribution of $B^0 \rightarrow \pi^0 \pi^0 K_S^0$ candidates. Points with errors show the data and events tagged as $q = +1$ and $q = -1$ are shown with filled and open circles together with the fit curves of solid and dashed lines, respectively.

5. $\sin 2\phi_1^{\text{eff}}$ measurement in CP -even states of $B^0 \rightarrow K_S^0 K_S^0 K_S^0$ decay

$B^0 \rightarrow K_S^0 K_S^0 K_S^0$ is a decay to three-body K_S^0 so that it is also the CP -even eigenstate induced by the penguin diagram. In BABAR, $\mathcal{S} = -0.94_{-0.21}^{+0.24} \pm 0.06$ has been reported that is away from zero by 3.8σ standard deviations [22]. Using full data set in the Belle, signal candidates of 329 ± 20 events are extracted from the fit as shown in Figure 5. Using the collected sample, CP violation will be measured in near future.

6. CP violation in $B^0 \rightarrow K_S^0 \pi^+ \pi^- \gamma$ decay

$B^0 \rightarrow K_S^0 \pi^+ \pi^- \gamma$ decay is induced via $b \rightarrow s \gamma$ penguin diagram. In scheme of the SM, no time-dependent CP violation is expected since photon polarization is limited to be left-handed by factor of fraction of s -quark mass over b -quark mass. Contribution of the new physics enhances right-handed component so that $\mathcal{S} \neq 0$ is expected. By comparing time-dependent CP violations

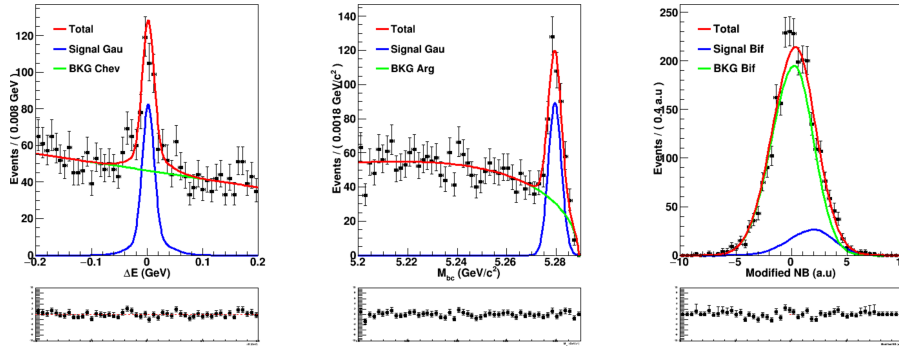


Figure 5: Distributions of M_{bc} , ΔE and modified neural-net output NB for selected $B^0 \rightarrow K_S^0 K_S^0 K_S^0$ candidates. Points with error bars show the data and curves show the fit result for signal yield extraction.

in symmetric region of Dalitz plane above and below the bisector of $s_{13} - s_{23}$, it leads to constraint Willson coefficients $\text{Re}(C'_7/C_7)$ and $\text{Im}(C'_7/C_7)$, where s_{13} and s_{23} are square of the invariant mass of $\pi^+ K_S^0$ and $\pi^- K_S^0$ system, respectively [23]. It can be accessible with order of integrated luminosity above 10 ab^{-1} which is accessible in Belle II but analysis is ongoing using Belle full data to establish analysis scheme.

7. Summary

In summary, we present recent measurements of the CP violation in the decays of $B^0 \rightarrow J/\psi\pi^0$, $B^0 \rightarrow \pi^0\pi^0 K_S^0$. We also show prospects of $B^0 \rightarrow K_S^0 K_S^0 K_S^0$ and radiative penguin studies that are on-going now. Statistical uncertainties are still dominant in most of those analyses and they are expected to be updated using the data from the Belle II [24] experiment in the future.

References

- [1] M. Kobayashi and T. Maskawa, Prog. Theor. Phys. **49**, 652 (1973).
- [2] Another naming convention, $\alpha(=\phi_2)$, $\beta(=\phi_1)$ and $\gamma(=\phi_3)$ are also used in the literature.
- [3] A. B. Carter and A. I. Sanda, Phys. Rev. Lett. **45**, 952 (1980); A. B. Carter and A. I. Sanda, Phys. Rev. D **23**, 1567 (1981); I. I. Bigi and A. I. Sanda, Nucl. Phys. **193**, 85 (1981).
- [4] A general review of the formalism is given in I. I. Bigi, V. A. Khoze, N. G. Uraltsev, and A. I. Sanda, “CP Violation” page 175, ed. C. Jarlskog, World Scientific, Singapore (1989).
- [5] A. Abashian *et al.* (Belle Collaboration), Nucl. Instr. and Meth. A **479**, 117 (2002); also see detector section in J. Brodzicka *et al.*, Prog. Theor. Exp. Phys. **2012**, 04D001 (2012).
- [6] S. Kurokawa and E. Kikutani, Nucl. Instr. and Meth. A **499**, 1 (2003), and other papers included in this Volume; T. Abe *et al.*, Prog. Theor. Exp. Phys. **2013**, 03A001 (2013) and references therein.
- [7] Z. Natkaniec *et al.* (Belle SVD2 Group), Nucl. Instr. and Meth. A **560**, 1(2006).
- [8] The Fox-Wolfram moments were introduced in G. C. Fox and S. Wolfram, Phys. Rev. Lett. **41**, 1581 (1978). The Fisher discriminant used by Belle, based on modified Fox-Wolfram moments (SFW), is described in K. Abe *et al.* (Belle Collaboration), Phys. Rev. Lett. **87**, 101801 (2001) and K. Abe *et al.* (Belle Collaboration), Phys. Lett. B **511**, 151 (2001).

- [9] S. H. Lee *et al.* (Belle Collaboration), Phys. Rev. Lett. **91**, 261801 (2003).
- [10] M. Feindt *et al.*, Nucl. Instr. Meth. A **654** 432 (2011).
- [11] D. J. Lange *et al.*, Nucl. Instr. and Meth. A **462**, 152 (2001).
- [12] R. Brun *et al.*, CERN DD/EE/84-1 (1984).
- [13] H. Kakuno *et al.*, Nucl. Instr. and Meth. A **533** 516 (2004).
- [14] H. Tajima *et al.*, Nucl. Instr. and Meth. A **533** 370 (2004).
- [15] C. Patrignani *et al.* (Particle Data Group), Chin. Phys. C, 40, 100001 (2016) and 2017 update.
- [16] Y. Amhis *et al.* (Heavy Flavor Averaging Group), Eur. Phys. J. C **77** 895 (2017).
- [17] Z. Xing, Phys. Rev. D **61** 014010 (1999).
- [18] T. Gershon and M. Hazumi, Phys. Lett. B **596** 163 (2004).
- [19] Y. Grossman and M. Woarh, Phys. Lett. B **395** 241 (1997).
- [20] H.-Y. Cheng, arXiv:0702252v1 [hep-ph] (2007).
- [21] B. Aubert *et al.* (BABAR Collaboration), Phys. Rev. D **76** 071101 (2007).
- [22] J. P. Lees *et al.* (BABAR Collaboration), Phys. Rev. D **85** 054023 (2012).
- [23] S. Akar *et al.*, J. of High Energy Phys. 09 034 (2019).
- [24] T. Abe *et al.* (Belle II Collaboration), arXiv:1011.0352 [physics.ins-det] (2010).